Comparison of Wave Measurements from a Synthetic Array Radar

J.R. Keeley

Marine Environmental Data Services Branch
Department of Fisheries and Oceans
Ottawa, Ontario, K1A 0E6

July 1982

Canadian Technical Report of Hydrography and Ocean Sciences No. 6

Fisheries and Oceans Pêches et Océans

Canada

Canadian Technical Report of Hydrography and Ocean Sciences

These reports contain scientific and technical information of a type that represents a contribution to existing knowledge but which is not normally found in the primary literature. The subject matter is generally related to programs and interests of the Ocean Science and Surveys (OSS) sector of the Department of Fisheries and Oceans.

Technical Reports may be cited as full publications. The correct citation appears above the abstract of each report. Each report will be abstracted in Aquatic Sciences and Fisheries Abstracts. Reports are also listed in the Department's annual index to scientific and technical publications.

Technical Reports are produced regionally but are numbered and indexed nationally. Requests for individual reports will be fulfilled by the issuing establishment listed on the front cover and title page. Out of stock reports will be supplied for a fee by commercial agents.

Regional and headquarters establishments of Ocean Science and Surveys ceased publication of their various report series as of December 1981. A complete listing of these publications and the last number issued under each title are published in the *Canadian Journal of Fisheries and Aquatic Sciences*, Volume 38: Index to Publications 1981. The current series began with Report Number 1 in January 1982.

Rapport technique canadien sur l'hydrographie et les sciences océaniques

Ces rapports contiennent des renseignements scientifiques et techniques qui constituent une contribution aux connaissances actuelles mais que l'on ne trouve pas normalement dans les revues scientifiques. Le sujet est généralement rattaché aux programmes et intérêts du service des Sciences et Levés océaniques (SLO) du ministère des Pêches et des Océans.

Les rapports techniques peuvent être considérés comme des publications à part entière. Le titre exact figure au-dessus du résumé du chaque rapport. Les résumés des rapports seront publiés dans la revue Résumés des sciences aquatiques et halieutiques et les titres figureront dans l'index annuel des publications scientifiques et techniques du Ministère.

Les rapports techniques sont produits à l'échelon régional mais sont numérotés et placés dans l'index à l'échelon national. Les demandes de rapports seront satisfaites par l'établissement auteur dont le nom figure sur la couverture et la page de titre. Les rapports épuisés seront fournis contre rétribution par des agents commerciaux.

Les établissements des Sciences et Levés océaniques dans les régions et à l'administration centrale ont cessé de publier leurs diverses séries de rapports depuis décembre 1981. Vous trouverez dans l'index des publications du volume 38 du *Journal canadien des sciences halieutiques et aquatiques*, la liste de ces publications ainsi que le dernier numéro paru dans chaque catégorie. La nouvelle série a commencé avec la publication du Rapport n° 1 en janvier 1982.

Canadian Technical Report of
Hydrography and Ocean Sciences 6

July 1982

COMPARISON OF WAVE MEASUREMENTS FROM A SYNTHETIC ARRAY RADAR

by

J.R. Keeley

Marine Environmental Data Services Branch
Department of Fisheries and Oceans
Ottawa, Ontario
K1A 0E6

Correct citation for this publication:

Keeley, J.R. 1982. Comparison of wave measurements from a synthetic array radar. Can. Tech. Rep. Hydrogr. Ocean Sci. 6:31 p.

©Minister of Supply and Services Canada 1982

Cat. No. Fs 97-18/6E ISSN 0711-6764

CONTENTS

	Page
Abstract	v
Résumé	v
Introduction	1
Data Sources	1
The Experiment	3
Waverider Data Analysis	5
Analysis of SAR Data	8
High Resolution Analysis	11
Low Resolution Analysis	23
Other Measurements	27
Discussion and Summary	27
Acknowledgements	30
References	31

ABSTRACT

Keeley, J.R. 1982. Comparison of wave measurements from a synthetic array radar. Can. Tech. Rep. Hydrogr. Ocean Sci. 6:31 p.

On September 1, 1981, synthetic array radar (SAR) data were collected over the ocean at a site about 350 km east of St. John's, Newfoundland. Simultaneous to the SAR collection were waverider buoy measurements of the wave field, and measurements of the winds. The SAR were analyzed using two-dimensional Fourier techniques to produce estimates of wave orientations and wavelengths. These estimates were then compared to wind measurements and one-dimensional spectra from the waveriders. Only the dominant peak in the waverider spectrum was seen in the SAR data but the wavelengths were in close agreement. Observed peak wavelengths in the SAR data agree with an adjustment of the wavefield to a changing wind direction.

RÉSUMÉ

Keeley, J.R. 1982. Comparison of wave measurements from a synthetic array radar. Can. Tech. Rep. Hydrogr. Ocean Sci. 6:31 p.

Le 1er septembre 1981, on a recueilli, à la surface de l'océan, à environnement 350 km à l'est de St. John's (Terre-Neuve), des données à l'aide d'un radar à ouverture synthétique (ROS). Au même moment, on prenait des mesures sur le champ des vagues au moyen d'houlographes et des mesures sur les vents. Les données fournies par le ROS ont été analysées en utilisant les techniques bidimensionnels de Fourier afin d'évaluer l'orientation et la longueur d'onde des vagues. On a comparé ces évaluations aux mesures des vents et aux spectres unidimentionnels enregistrés par les houlographes. Seule la partie dominante du spectre du houlographe a été observée dans les données fournies par le ROS; cependant, il y avait une étroite concordance des longueurs d'onde. Dans les données fournies par le ROS, les longueurs d'onde les plus élévées coincident avec le rajustement du champ des vagues au changement de direction du vent.

INTRODUCTION

The Government of Canada has been sponsoring a study to determine the merits of launching a satellite in the late 1980's, primarily to monitor ice and ship traffic in the Canadian arctic archipelago. The main sensor is to be a synthetic array radar (SAR) because of its ability to supply useable data with little regard to atmospheric conditions or the availability of sunlight. As part of the study, a variety of scientific teams were formed from different disciplines to investigate the usefullness of SAR data. One of the studies of the oceanographic team was to compare ocean wave date returned from a SAR to more conventional measurements.

Although there are a number of published studies describing the ability of a SAR to image ocean waves (e.g. Hsiao 1978 ; Beal 1980; Alpers, Ross and Rufenach 1981) the mechanism by which this occurs is not well understood (Vesechy and Stewart 1982 give an excellent review). Because of this, only wavelength and orientation of waves are readily derivable from SAR data at present. Until recently, the analyses were conducted using optical techniques. With the development of digital SAR's however, has come the capability of using computers in direct analysis of the data.

An overall objective of the oceanographic study team is to increase the familiarity of Canadian oceanographers with SAR data. This is important because these data are relatively new; therefore, the knowledge of their handling and use is not widespread. More specifically, the purpose of the study described here was to make comparisons of wavelengths and orientations derived from a SAR with those derived from more conventional instruments. Analyses such as these have been done by others (see for example the earlier cited references) so that the results presented here extend the variety of wind and wave conditions for which comparisons have been done.

DATA SOURCES

There are at least three sources from which data for wave comparisons may be drawn. One of these is the SAR data collected by the SEASAT satellite while it was operating. The SAR onboard provided a large amount of data even though it was only working for about three months of 1978. A significant fraction of these data have still not been processed digitally.

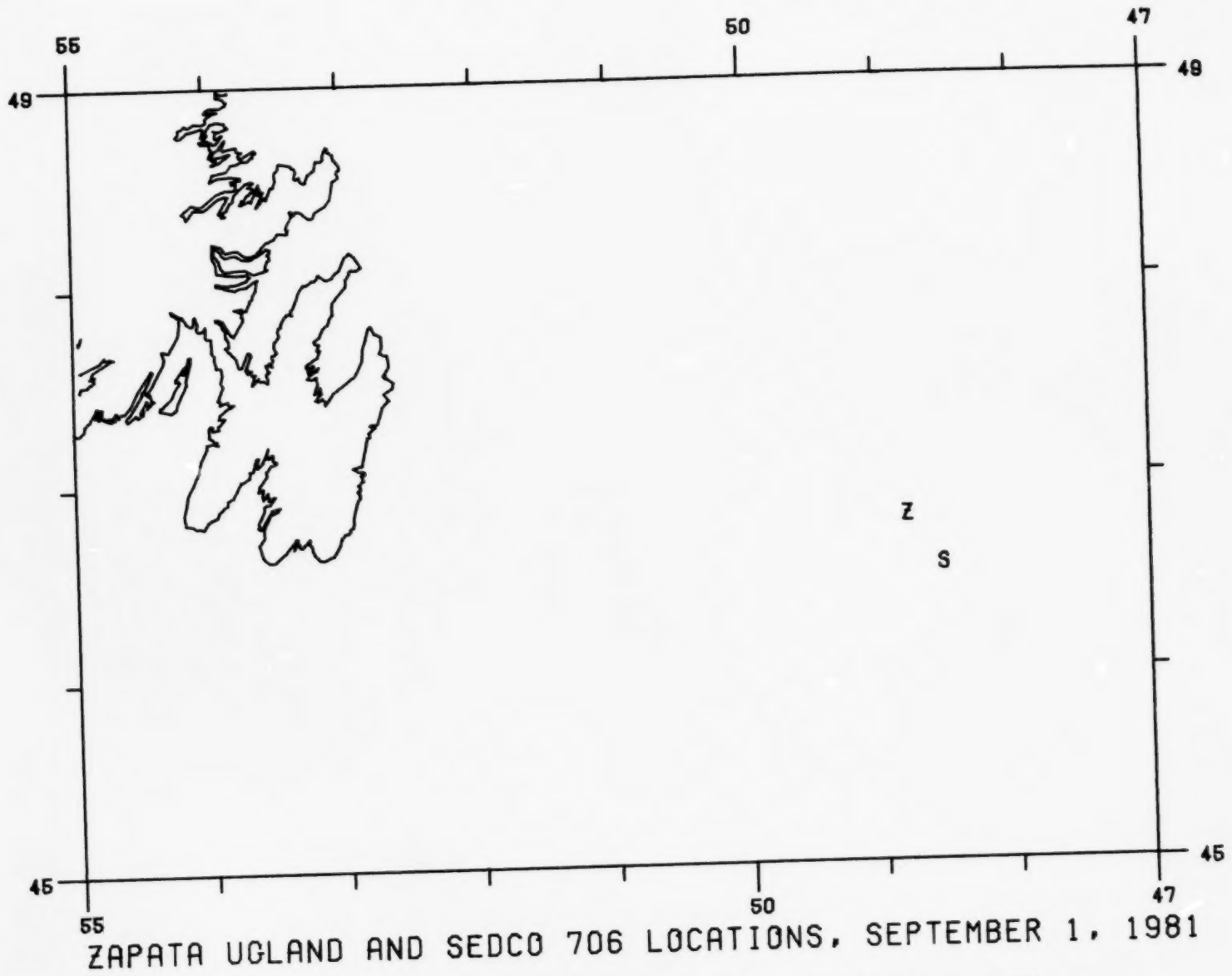

Figure 1. Map showing the locations of the Zapata Ugland (Z) and Sedco 706(S) rigs on September 1, 1981.

Another source of SAR data is to use the instrument mounted on an aircraft and operated by the Canada Centre for Remote Sensing (CCRS). This SAR was made available to each of the study teams. The oceans team received one flight in September of 1981 and two more in March of 1982.

Independent of the SAR data is the wave information compiled by the Marine Environmental Data Services (MEDS) Branch of the Department of Fisheries and Oceans of the Canadian government. Buoys have been used to obtain surface elevation records from sites off the east, west and northern coasts of Canada (Wilson and Baird 1981). A number of these sites were operating coincidently in time and location to SAR data obtained from SEASAT.

The increased offshore activity off the coasts of Canada by oil companies has highlighted the requirement for more knowledge of oceanographic conditions for environmental impact statements and safety. Part of the requirements to obtain operating permits has been to gather wave information often by using MEDS waverider buoys. The offshore rigs offer an excellent open ocean location at which both wind and wave measurements are available. The aircraft flight of 1981 flew over two platforms both having operating waverider buoys. A discussion of the analysis of data from this experiment forms the body of this report. Analyses utilizing the data from SEASAT must wait until the data become available.

THE EXPERIMENT

The experiment with the CCRS airborne SAR was scheduled for the fall of 1981 over waverider buoys positioned close to drilling rigs off the east coast of Canada. The aircraft flew the mission on September 1, 1981 over the Zapata Ugland and Sedco 706 rigs positioned as shown in Figure 1. This site was chosen for the experiment because the rigs were about 350 km east of Newfoundland and consequently there was little sheltering of waves from any direction. The rigs were in about 70 m of water so that only long waves would experience the effects of refraction. Because this was the first experiment, it was desirable to ensure some redundancy by having two waveriders very close to each other and which could be covered on a single flight. The two waveriders also allowed comparisons between them as a further check of the instrument performance.

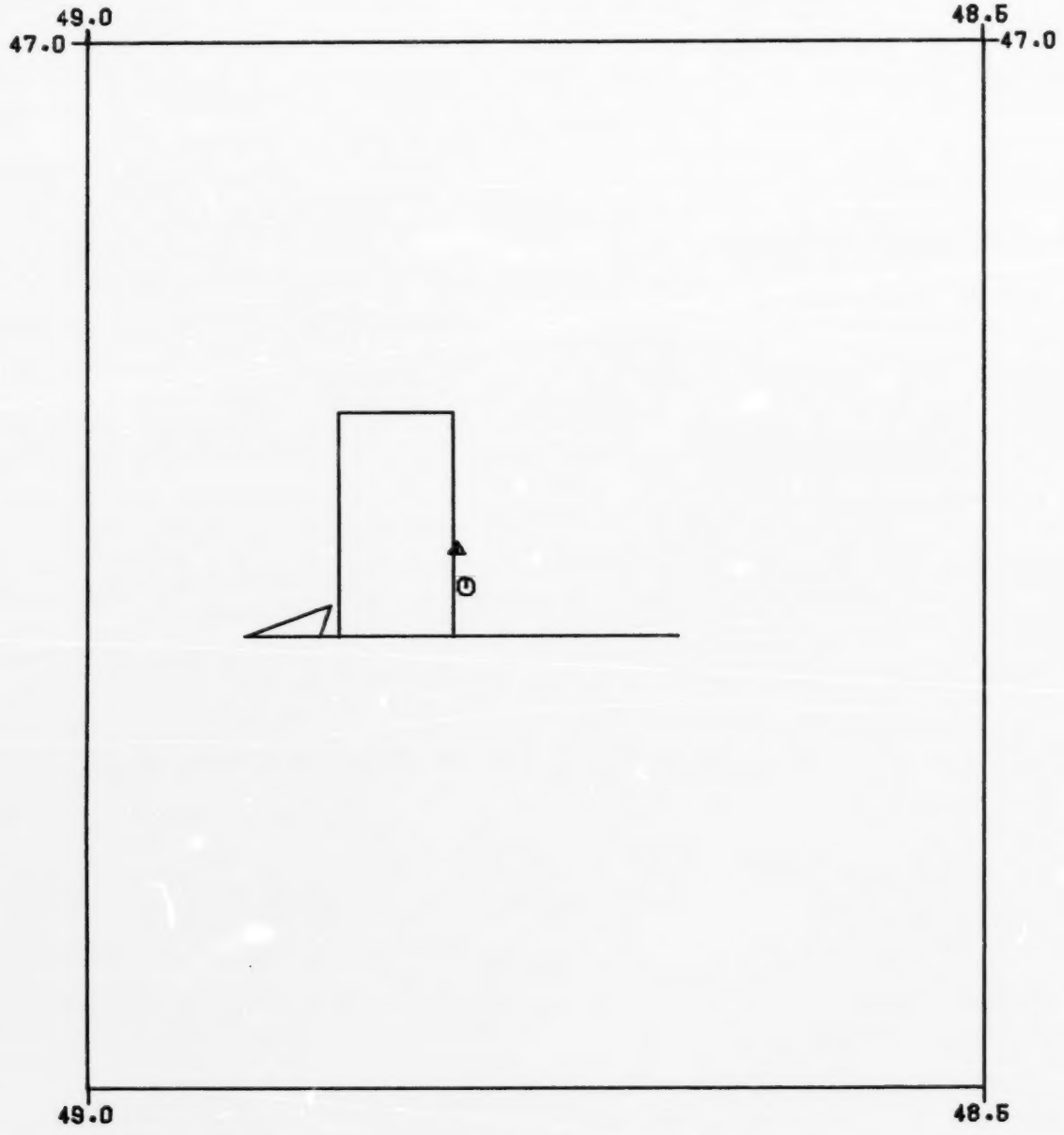

Figure 2: The orientation of the analysed SAR scene with the rig (0) and waverider (Δ) marked. Note that the azimuth direction is along the flight line and the range is north.

The aircraft flew a box pattern at an altitude of 3100 metres about each rig with the SAR looking into the box. The near depression angle was 90° from the horizontal and the far angle was about 15°. The SAR operated at both C(5.35 GH_z) and X(9.35 GH_z) band with vertical-vertical polarization.

The aircraft had a real time processor (RTP) on board which gave an immediate SAR image of the ocean surface. The RTP strip image of the entire flight was examined to find a scene to be processed and which appeared to show surface waves. The scene chosen was from the westward leg around the Zapata Ugland as shown in Figure 2. This scene was extracted from the digital SAR data recorded by the aircraft and geometrically corrected so that each pixel (picture element) represents a 3 m by 3 m patch of the ocean surface. The resulting scene was approximately 12 km by 12 km of the ocean surface. This processing was carried out by the Communications Research Centre (CRC) of the Department of National Defence in Ottawa.

Both C and X band images were processed. Because of the amount of data, each scene was split and each half was written onto a magnetic tape. The C band data did not show on the RTP, and when it was processed looked almost uniformly grey (Figure 3). This poor return was attributed to focusing problems in the radar (R.K. Raney, personal communication). The X band scene (shown in Figure 4) reflected what was seen in the RTP. Nearly all of the results discussed here apply to this X band scene.

WAVERIDER DATA ANALYSIS

The waverider buoys used by MEDS are of the floating accelerometer type manufactured by Datawell. It is the practice at MEDS to verify the calibration of each buoy at five frequencies ranging from 0.3 to 0.05 hz before installation at a station and after it is removed. The output must be within 3% of accurate for wave periods from 2 to 20 seconds and within 10% of accurate at a wave period of 27.5 seconds. The buoys used in this experiment operated within these specifications.

The usual recording procedure is for the buoy to sample water elevation every 0.1 seconds for 20 minutes out of every 3 hours. However, at the Zapata Ugland rig, the buoy was recording continuously as the SAR was operating. The aircraft flew the western leg of the box from 2208 to 2218 GMT.

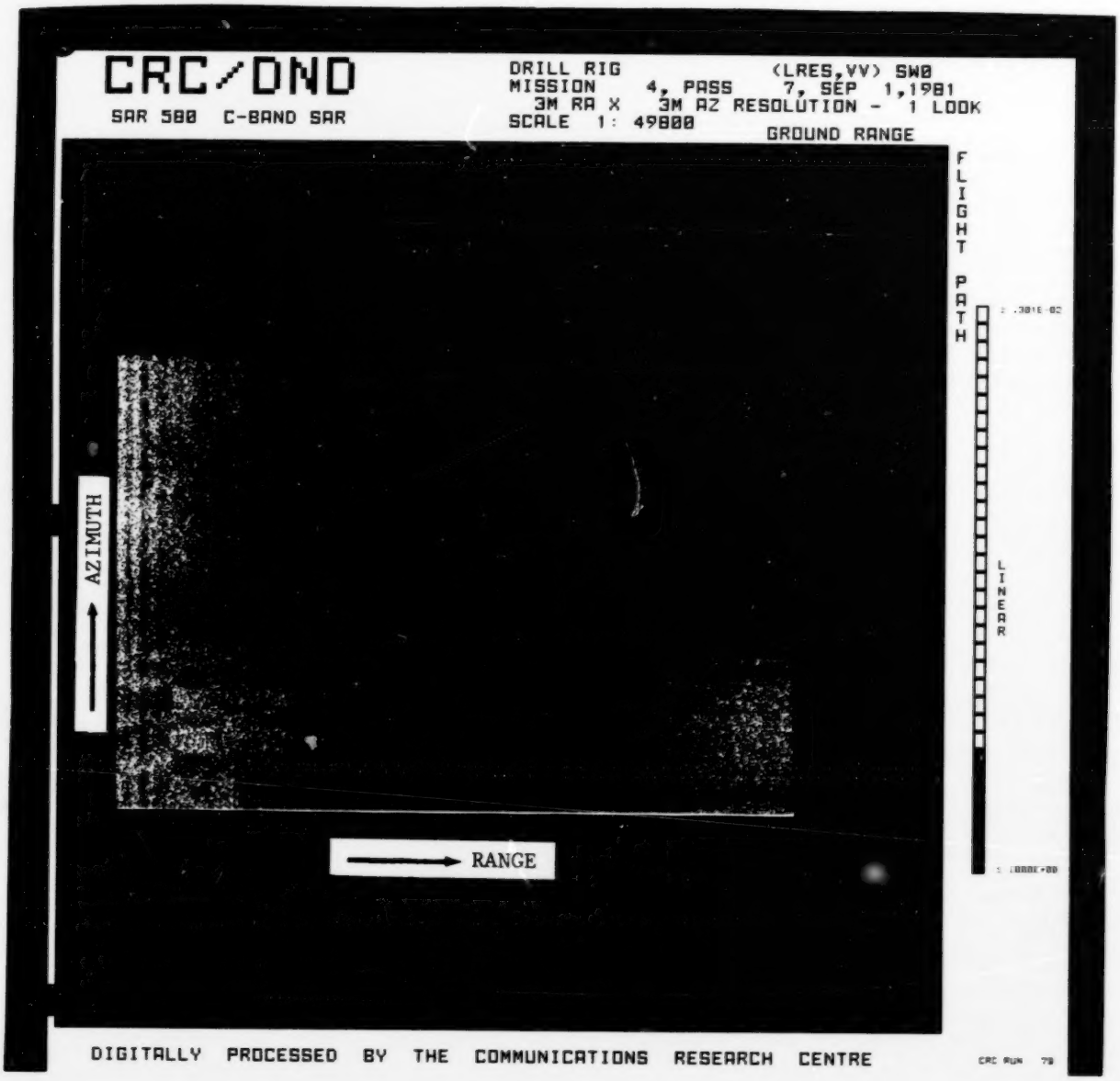

Figure 3: C band SAR imagery

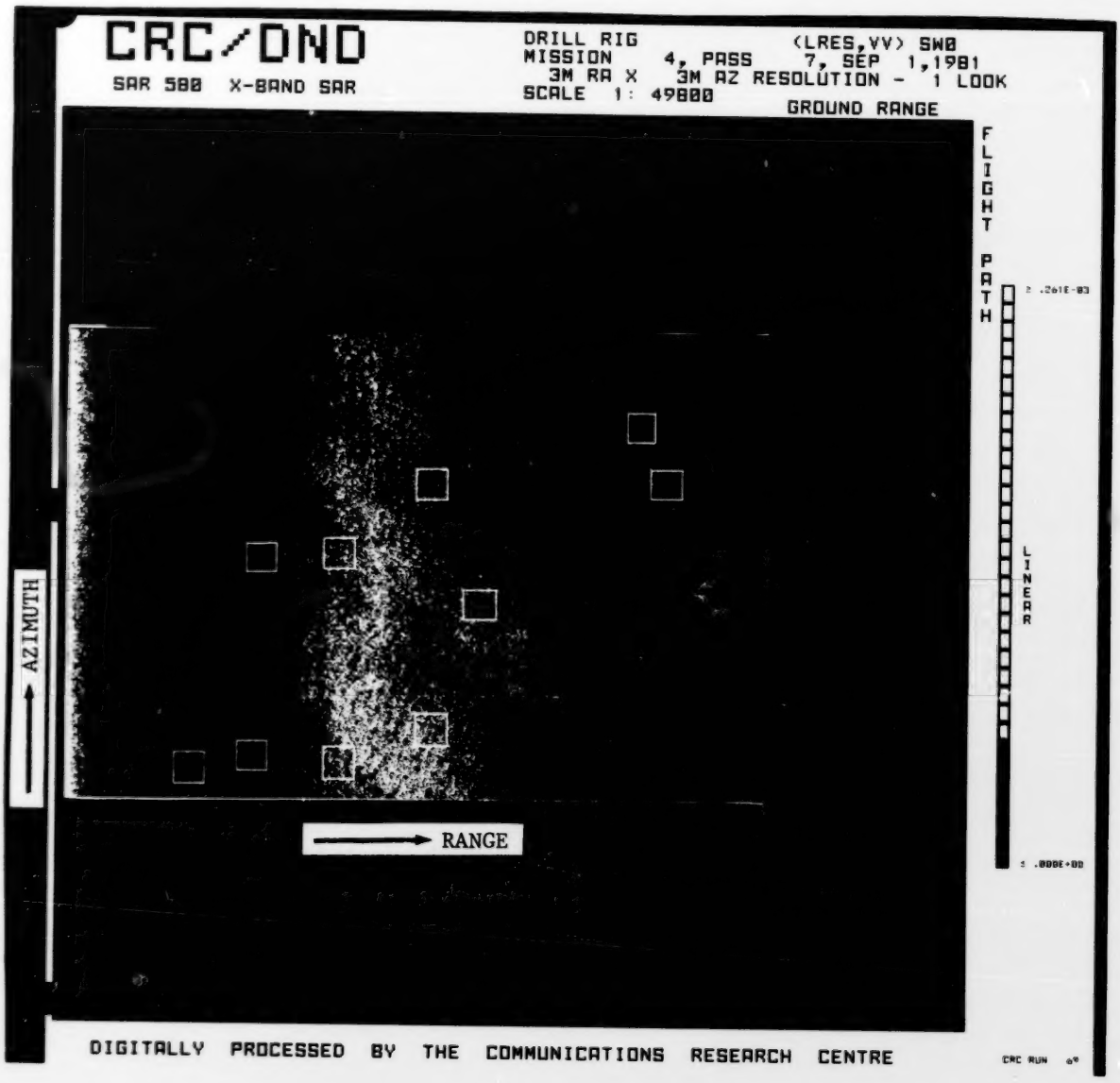

Figure 4: X-band SAR imagery. The ten white boxes are the subscenes analyzed.

The waverider data were analysed in two different ways to provide independent spectral estimates. The first way was to employ the usual Fourier techniques used by MEDS in the analysis of its wave records. Each 20-minute record was subsampled at approximately 0.5 sec., and the resulting time series was broken into 8 blocks of 1024 points each. Spectral estimates were calculated for about 60 frequency bands between 0.05 and 0.5 hz. The 8 spectra were then averaged in each band to provide smoother estimates. The frequency spectrum was then converted to a wavenumber spectrum by using the general dispersion relation for surface waves.

The second technique employed was to use the maximum entropy techniques (ME) as described by Ulrych and Bishop (1975). The key element in an ME analysis is to choose the correct length of the prediction error filter. This choice was made by setting the filter length to be very long and computing the length at which the final prediction error (Ulrych and Bishop 1975) was minimized. This was done for all of the records available. Nearly all of the final prediction errors grouped about a single filter length. The filter length was set by averaging all of the values and this was then used in all subsequent computations. Again, the calculated frequency spectra were converted to wavenumber spectra by using the surface wave dispersion relation.

The westward leg of the flight was made between 2206 and 2209 GMT. The 20-minute period used from the waverider data was that from 2200 to 2220 GMT. All comparisons to the SAR data will be shown for this time only. The waverider derived spectra from other times, before and after, show similar characteristics.

ANALYSIS OF SAR DATA

The central calculation of the wavelength and orientation characteristics of ocean waves in a SAR scene employs a two-dimensional Fourier transform computation. This requires the manipulation of an N by N matrix and, hence, may result in substantial memory requirements of a computer. There are, however, other factors to be considered before the choice of N is made. It is desirable to make N as large as possible to provide adequate definition of the longer wavelength components in the scene and preserve maximum resolution. But, if most of the energy is in longer wavelengths, it is not necessary to maintain the highest resolution provided by the data. Thus, N may be kept at reasonable values in terms of computer resources by using low pass filtering techniques at the cost of degraded resolution.

The spectra derived from the waverider data showed two peaks, one at about 25 m wavelength and the more energetic one at about 145 m. As the first analysis, it was decided to set N to be 128 and to process data at the highest resolution, 3 m.

The SAR data supplied by CRC consisted of values of the strength of the radar return in floating point numbers rather than being partititioned into some arbitrary grey scale. The data supplied is called one look resolution since it is the highest derivable from the instrument, but it also tends to be noisy. Since subscenes of 128 by 128 pixels were to be analysed, it was decided to select 10 subscenes from the main scene and to use averaging techniques to reduce the noise.

The first step in the analysis was to choose the 10 subscenes. Initially, subscenes from the light band in the centre of the scene were chosen by looking for areas with well developed wave patterns. Subsequently, the scenes from the darker areas were chosen with the aid of a random number generator. These are outlined in Figure 4. Each subscene was then extracted from the data tape and characteristics such as mean, variance and noise were calculated. The means were of interest since the subscene showed large variations from the centre to the edges while the noise could be used to estimate how many grey shades would be adequate to represent the subscene. (Details concerning the computer routines used and the analysis procedures are available in Hanebury and Keeley 1982). The variance was used in normalizing the radar return in each subscene. The estimate of noise in the subscene is done by differencing values in adjacent pixels by rows and by columns. These differences are then squared and averaged to get an estimate of the standard deviation of the noise at successively greater differences. This technique magnifies noise and suppresses signals more or less effectively depending on the scale of variation of the signal. It was found that about 20 differences were required before the noise estimate showed relatively small changes as the number of differences increased.

Table 1 summarizes the noise estimates and required grey shades to represent the data from 10 X-band subscenes and 5 C-band subscenes. The most evident characteristics are that the noise is about one order of magnitude smaller for the X over the C band subscene; however, the maximum value in the C band is about one order of magnitude larger than in the X band, while the minima in the two bands are about the same. The number of grey levels required was estimated to be the ratio of the difference of the maximum and minimum to the standard deviation of the noise. As is shown in

Table 1. Statistical characteristics of selected subscenes.

Azimuth	Range	Frequency	Minimum ($\times 10^{-7}$)	Maximum ($\times 10^{-4}$)	Mean ($\times 10^{-5}$)	Standard Deviation ($\times 10^{-5}$)	Noise ($\times 10^{-5}$)	Grey Shades
250	1500	X	4.14	3.96	9.60	5.20	1.47	26
790	1700	X	1.12	2.92	7.57	4.16	1.14	26
1300	1500	X	5.63	2.88	7.19	3.83	1.10	26
100	1100	X	6.49	3.36	8.45	4.66	1.38	24
1000	1100	X	5.89	3.46	8.06	4.40	1.37	26
126	727	X	1.80	1.72	4.48	2.36	0.72	24
1553	2397	X	3.63	1.93	4.78	2.53	0.72	26
981	765	X	5.41	1.68	4.58	2.43	0.71	24
71	453	X	2.63	1.77	4.99	2.60	0.74	24
1311	2512	X	8.91	1.79	4.55	2.35	0.69	26
600	600	C	60.30	23.00	67.60	34.00	11.10	21
1000	1500	C	36.70	18.80	56.30	29.10	10.70	18
800	2200	C	29.70	21.60	60.90	31.80	12.20	18
1400	800	C	67.40	19.60	57.00	29.40	10.50	19
1800	1800	C	32.70	20.20	59.00	31.10	11.90	17

Table 1, the number of grey shades in both C and X band are approximately the same. Thus, even though the X and C band subscenes look much different qualitatively, the difference does not lie in one being significantly noisier relative to the signal.

An examination of the distributions of values in X and C band subscenes does show differences. Although both are skewed, the X band subscenes have a sharper peak, shown by a smaller standard deviation, and a relatively more elongated tail than seen in the C band subscenes. This may be reflecting the uniformity of the C band image as compared to the X band.

HIGH RESOLUTION ANALYSIS

The 10 subscenes from the X band subscene were processed initially at the highest resolution. Thus, a matrix of 128 by 128 pixels had an areal equivalent to 384 by 384 metres. The two-dimensional Fourier transform was done by extending traditional one-dimensional techniques. Before calculating the transform, a plane was fitted in a least squares way to the subscene and then the plane was removed; this eliminated any trends. Next, to calculate a smoother transform, a Hann type taper was applied to the entire subscene. Effectively the value in each pixel was multiplied by a cosine, positioned over the subscene such that the value was zero at the edges and one in the exact centre. The two-dimensional Fourier transform was then calculated using standard methods.

The resulting transforms from each subscene were still very noisy. In order to reduce this noise, it was decided to average transforms from all 10 subscenes. The power in each transform, however, was strongly dependent on from where the original subscene was chosen. Thus, subscenes from bright parts of the scene had more power than those from darker positions. To remove this bias in the averaging, each transform was normalized by the calculated variance in the subscene from which it was derived. The transforms were then averaged.

Two different techniques were used to display the two-dimensional transform. The first (shown in Figure 5) was a simple contouring of values. To reduce the clutter, only 10 contour levels were used. These levels were chosen to emphasize the values near the maximum by fitting one decade of a log scale to the difference between the maximum

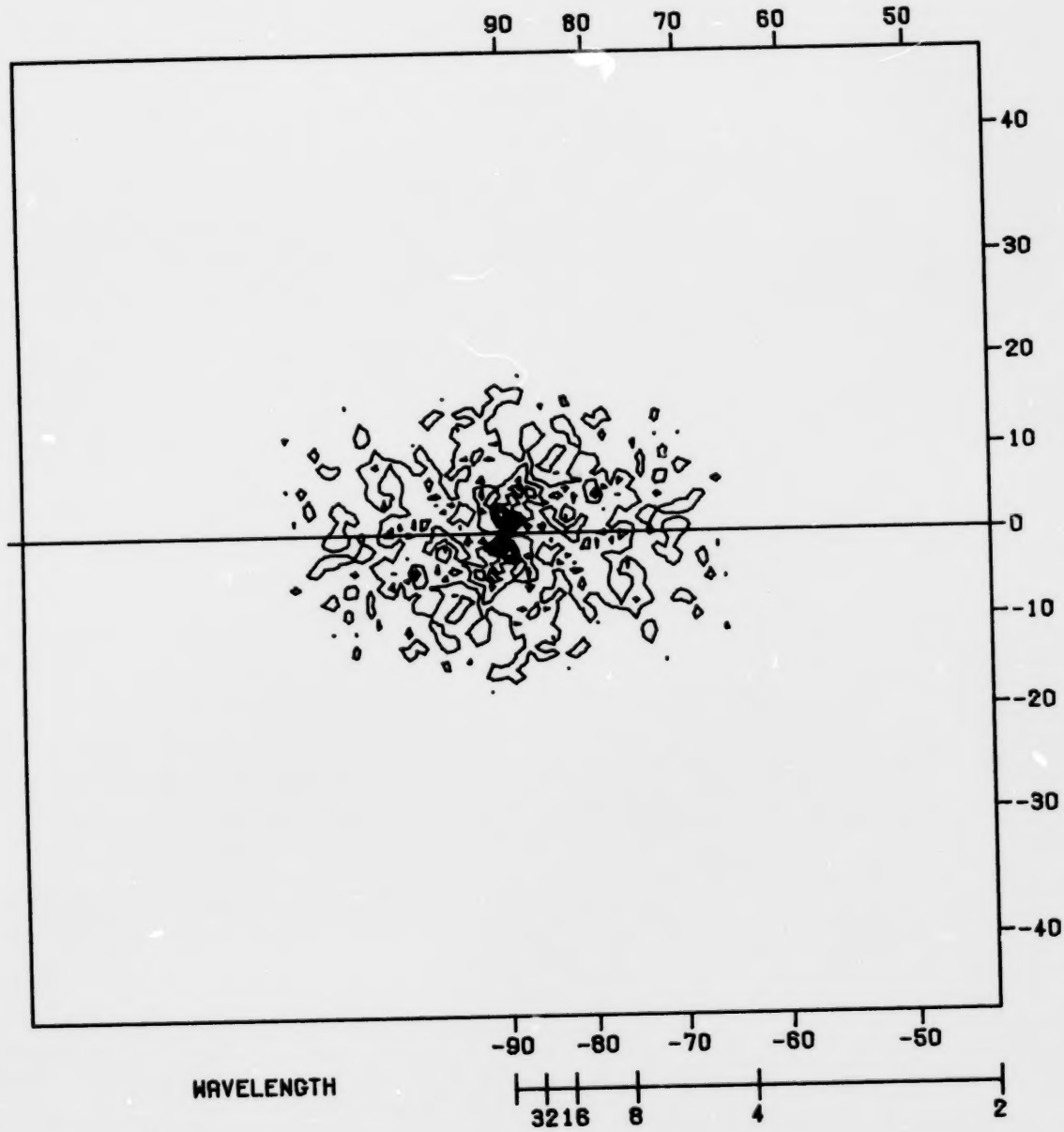
90
80
70
60
50
40
30
20
10
0
-10
-20
-30
-40
-90
-80
-70
-60
-50
WAVELENGTH
32
16
8
4
2
SAR 580 81-66-X1 AVERAGED FFT FOR 10 SCENES RES=3

Figure 5

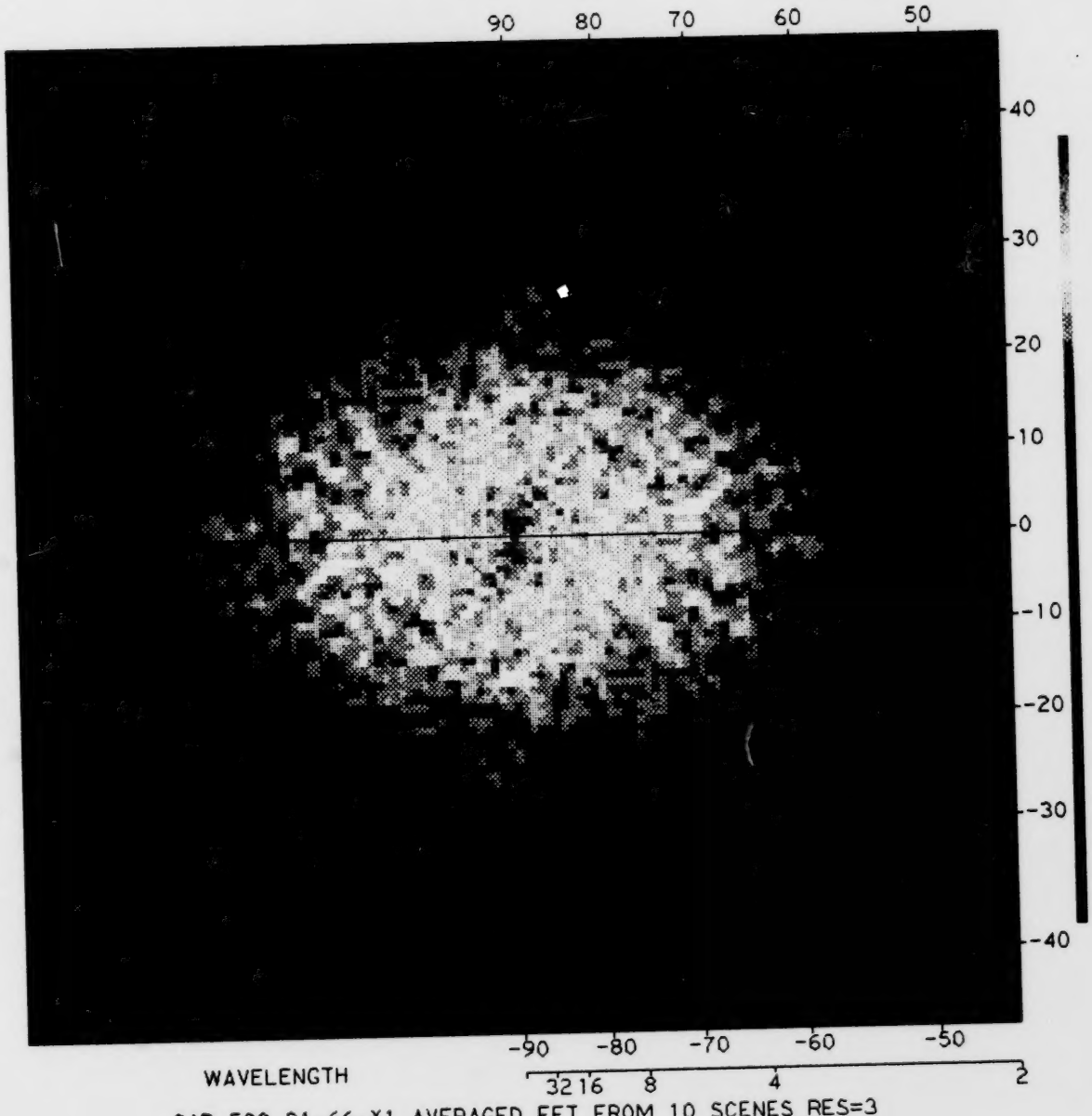
90 80 70 60 50
40
30
20
10
0
-10
-20
-30
-40
-90 -80 -70 -60 -50
WAVELENGTH
32 16 8 4 2
SAR 580 81-66-X1 AVERAGED FFT FROM 10 SCENES RES=3

Figure 6

and minimum value in the transform. The contour levels then corresponded to the integral divisions in the decade. Because of the large range of values, this type of display can become cluttered by details.

A second display was made using a colour plotter driven by computer. Figure 6 shows the same information displayed in this way but now with more colour levels. Again the same type of non-linear scale was used. Such a display is much more effective in presenting the information. The scale at the bottom of Figure 6 can be used to determine the wavelength of any feature in the transform. This is done by measuring the radial distance from the centre of the transform to the feature and by using the scale to convert this distance to a number on the scale. This number is multiplied by the resolution factor to find the wavelength.

The transform shown in Figure 6 still looks noisy but there are some features which can be seen. The transform is oriented with respect to the original subscene such that O° is to the east (or west because of the 180° ambiguity in the calculation of the transform).

An inspection of Figure 6 shows the strongest peak at 90° and only 2 pixels from the centre. At this long a wavelength, the directional resolution is poor as is the determination of wavelength. However, in the region within 5 pixels of the centre of the transform, there is a diffuse peak with a directional tendency at 70° to 80°. At shorter wavelengths there appear to be three other peaks at 72° and 53m, 12° and 48m, 20° and 29m.

The final stage in the analysis is to make a comparison of the wavelengths of the peaks in the two-dimensional transform from the SAR to the one-dimensional spectrum calculated from the waverider data. This can be done by picking off peaks as before, or by folding up the two-dimensional transform into one dimension and making a straight comparison to the waverider spectrum. The transform is folded by adding all of the values in bands at varying radial distances from the centre. These values are then scaled by the area of the annulus from which they were summed. The result is shown in Figure 7. The amplitude of the peaks in the one-dimensional SAR transform have not been related to the height of the waves. However, it does appear that higher waves produce stronger peaks. The 95% confidence intervals have been shown on the three curves. Notice that for the SAR, this interval is dependent upon the wavelength because

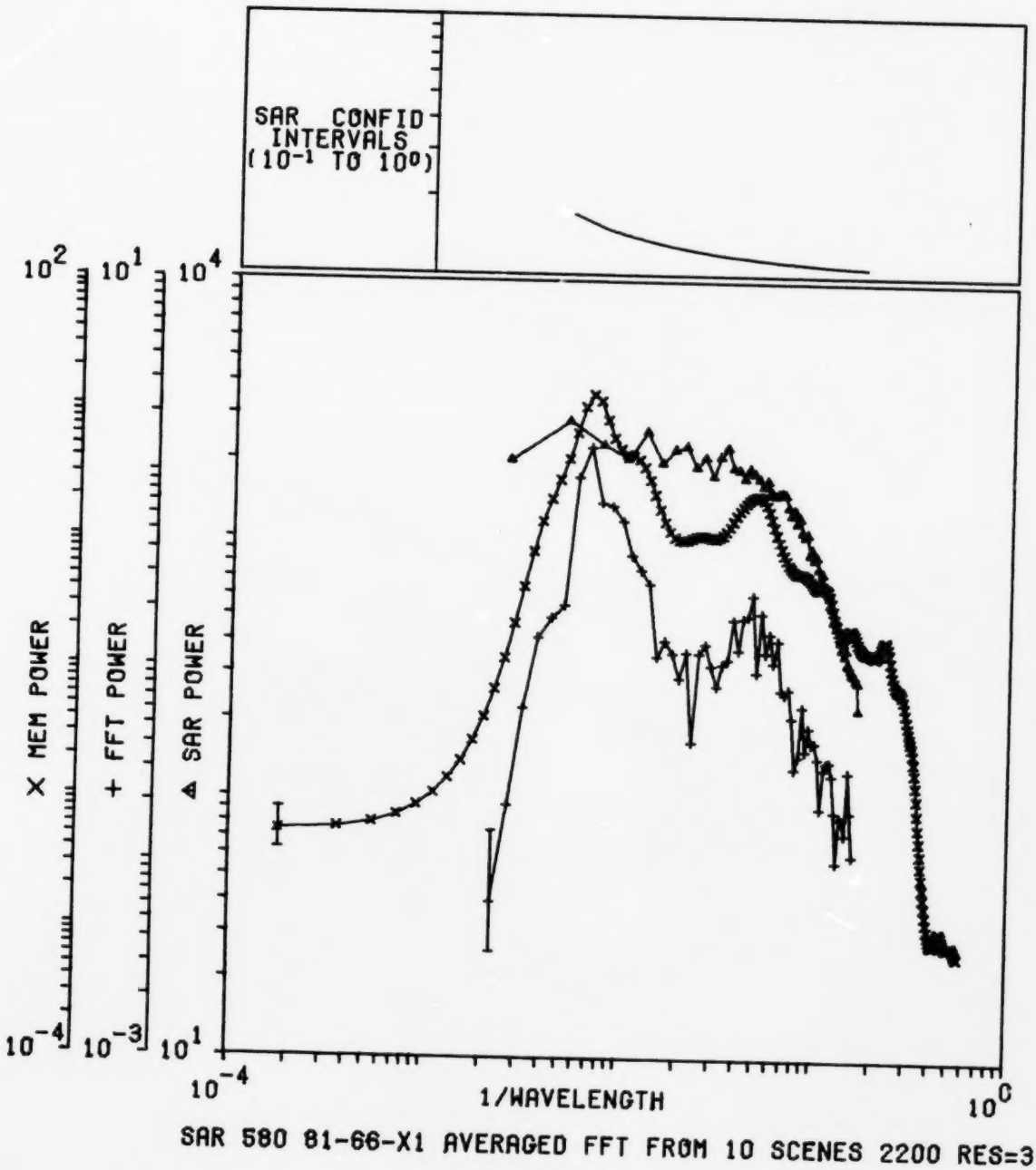
SAR CONFID
INTERVALS
(10-1 TO 10⁰)
10²
10¹
10⁴
X MEM POWER
+ FFT POWER
Δ SAR POWER
10⁻⁴
10⁻³
10¹
10⁻⁴
1/WAVELENGTH
10⁰
SAR 580 81-66-X1 AVERAGED FFT FROM 10 SCENES 2200 RES=3

Figure 7

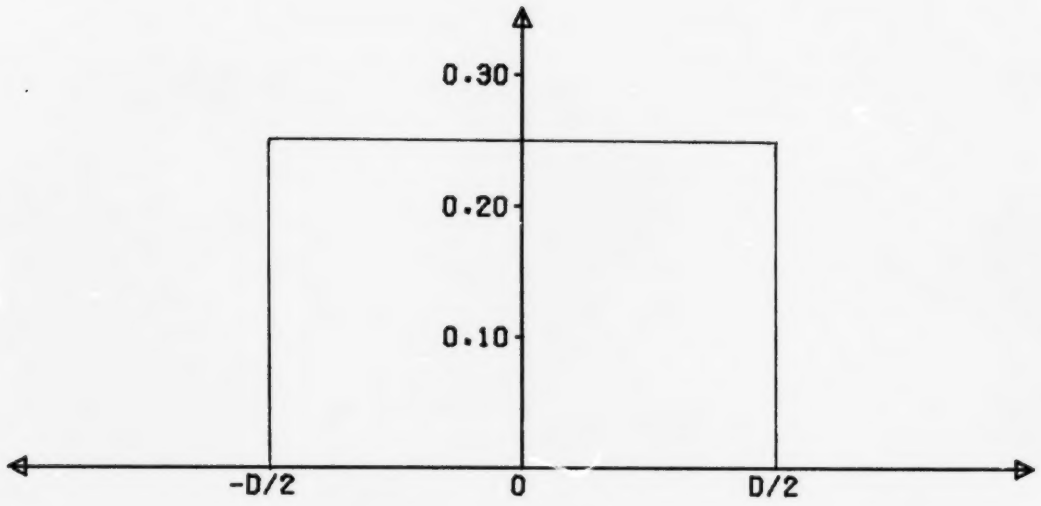

Figure 8a: BOXCAR FILTER WEIGHTS W(D)

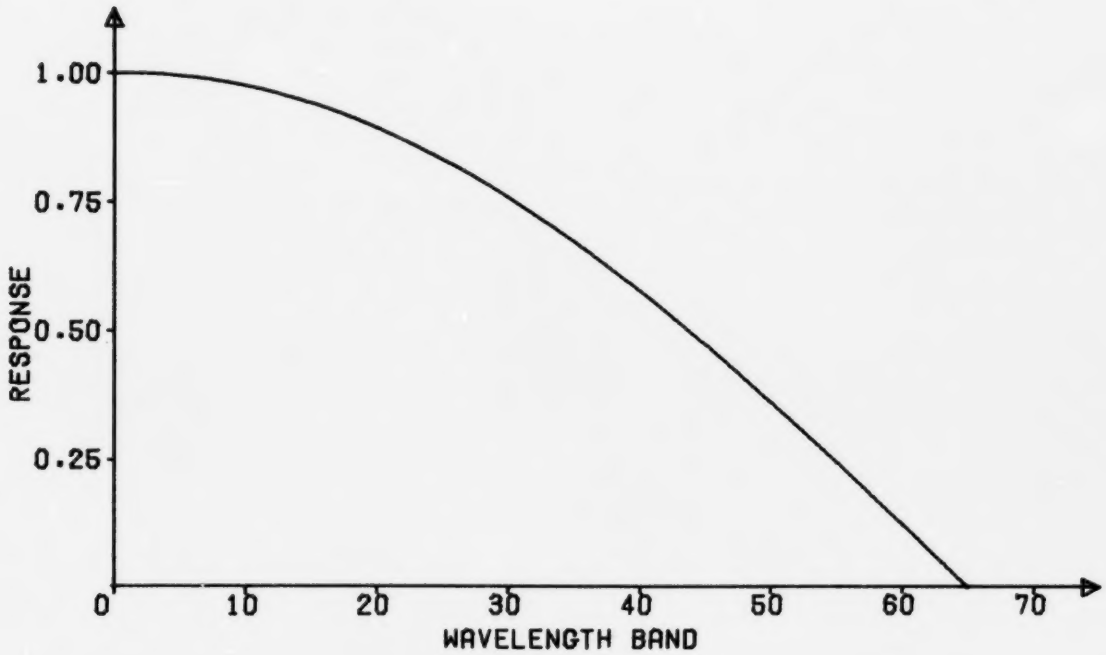

Figure 8b: BOXCAR FILTER RESPONSE FUNCTION R(F)

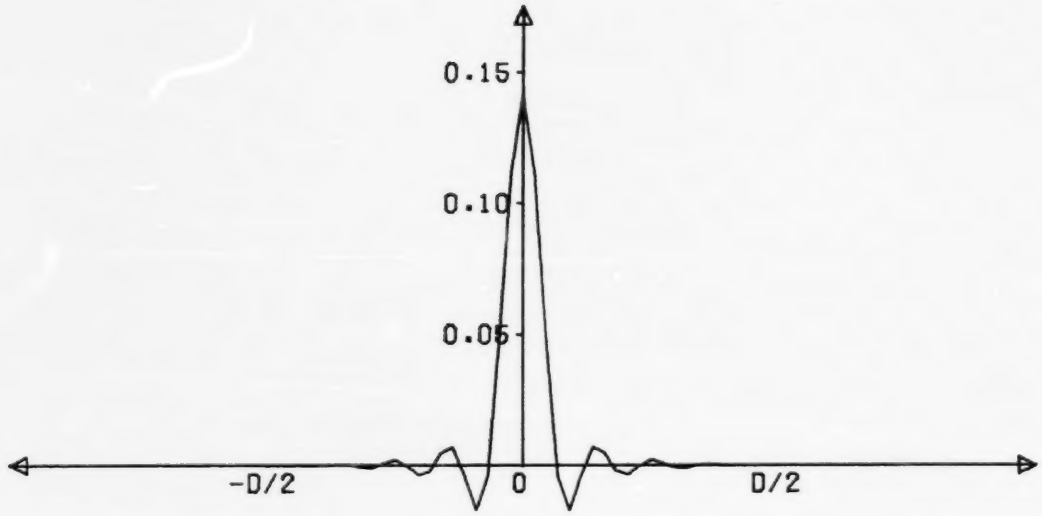

Figure 9a: CARTWRIGHT FILTER WEIGHTS W(D)

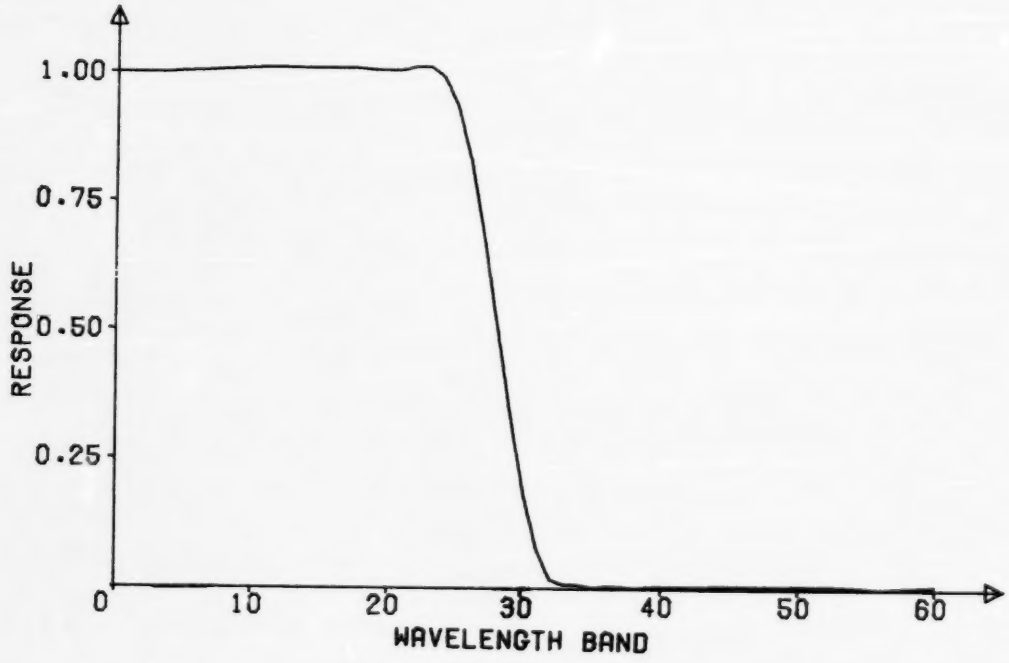

Figure 9b: CARTWRIGHT FILTER RESPONSE FUNCTION R(F)

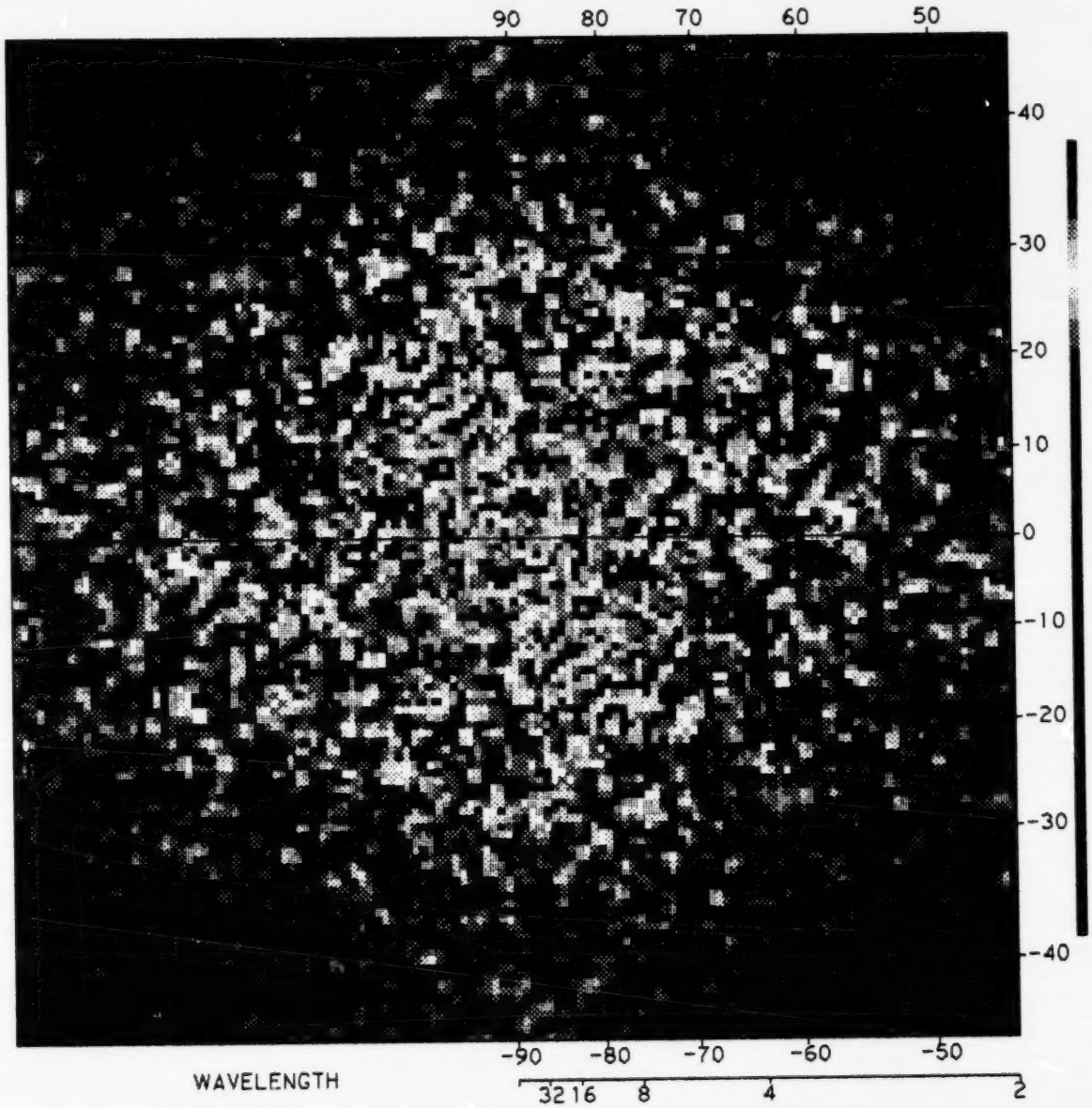
90 80 70 60 50
40
30
20
10
0
-10
-20
-30
-40
-90 -80 -70 -60 -50
WAVELENGTH
32 16 8 4 2
SAR 580 81-66-X1 BOXCAR FILTER AZ=790 RG=1700 DEC=2 RES=6

Figure 10

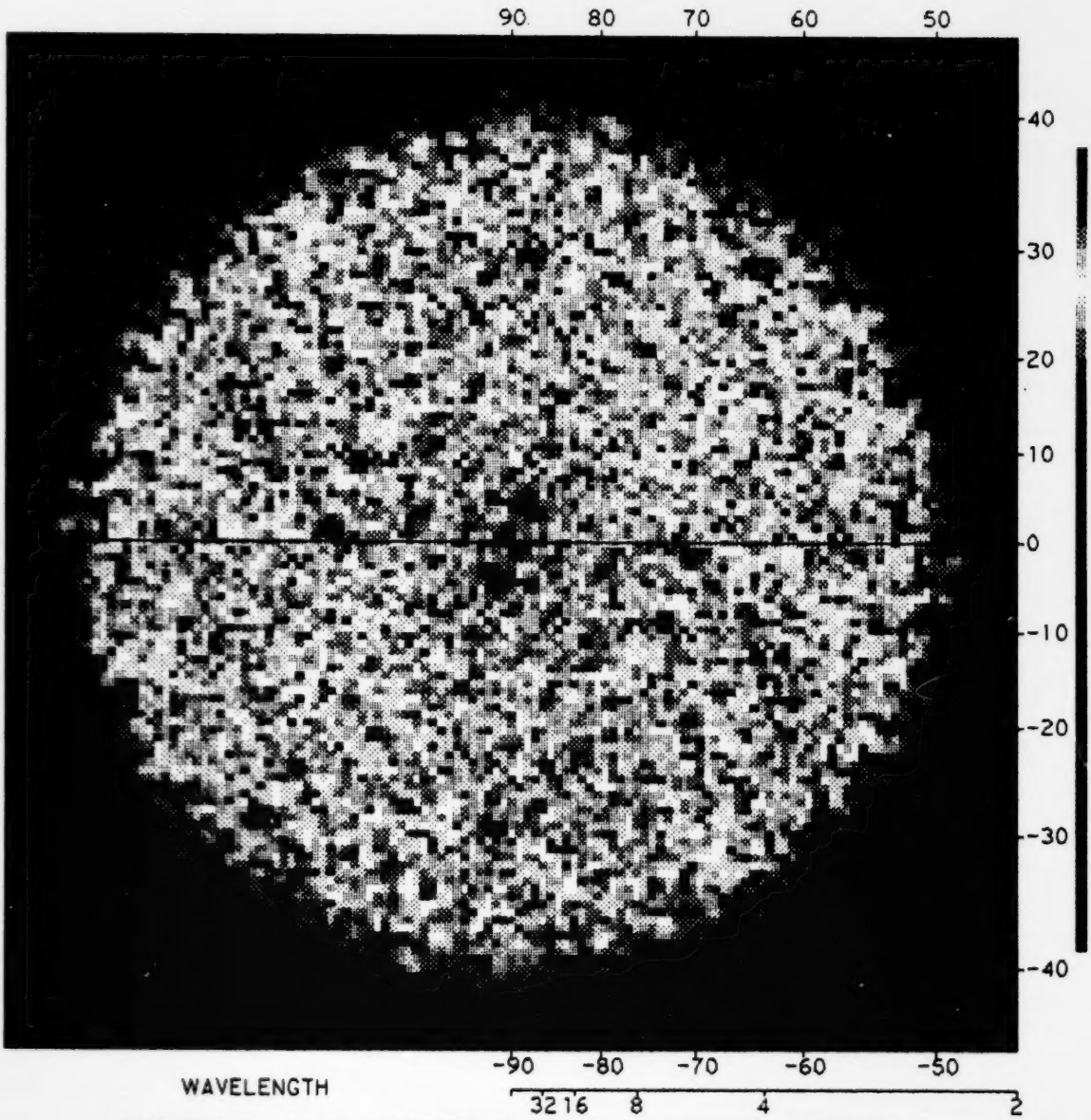
90 80 70 60 50
40
30
20
10
0
-10
-20
-30
-40
-90 -80 -70 -60 -50
WAVELENGTH
32 16 8 4 2
SAR 580 81-66-X1 CARTWRIGHT AZ=790 RG=1700 DEC=2 RES=6

Figure 11

of the varying number of values which compose the estimates at each wavelength. An examination of the SAR curve shows virtually no peak which stands above the 95% interval. Of the three peaks identified explicitly, none shows any relation to peaks in the FFT or MEM spectra. In particular, the secondary peak at about 20 m does not show up in the SAR. The main peak of the waverider spectrum occurs at too long a wavelength to be properly resolved in this analysis.

LOW RESOLUTION ANALYSIS

Because the analyses of the scenes at the highest resolution did not allow the adequate definition of long wavelengths, it was necessary to improve the definition. This was accomplished by applying a two-dimensional low pass filter to the selected subscenes, decimating the output and applying the same analysis techniques as before. A computer program was written to transform well known one-dimensional filters to their two-dimensional counterpart having the same response characteristics. Details of the program are given in Hanebury and Keeley (1982) and Taylor (1982). The outputs of two of the filters will be shown to illustrate the techniques but only one is used in subsequent analyses.

The chosen filters were the boxcar and the Cartwright. The two-dimensional Cartwright filter was generated using the techniques described by Taylor. The boxcar filter was simply to average values in a box 2 by 2 pixels in size. This averaging degrades the resolution by a factor of 2, the same factor chosen for the Cartwright filter. Figures 8 and 9 show the weighting and response functions of these two filters as they are applied to the two-dimensional subscene. Both filters have isotropic directional properties.

The same subscene has been analysed using both filters and the Fourier transforms of each are shown in Figures 10 and 11. As predicted by the filter response functions, the Cartwright filter shows a much more uniform transform to the wavelength at which the filter cuts off.

The Cartwright filter was used on the same 10 subscenes as previously chosen. The subscenes were chosen such that after filtering they were centered on the same subscenes that are shown in Figure 4. The two-dimensional Fourier transforms are shown in Figures 12 and 13.

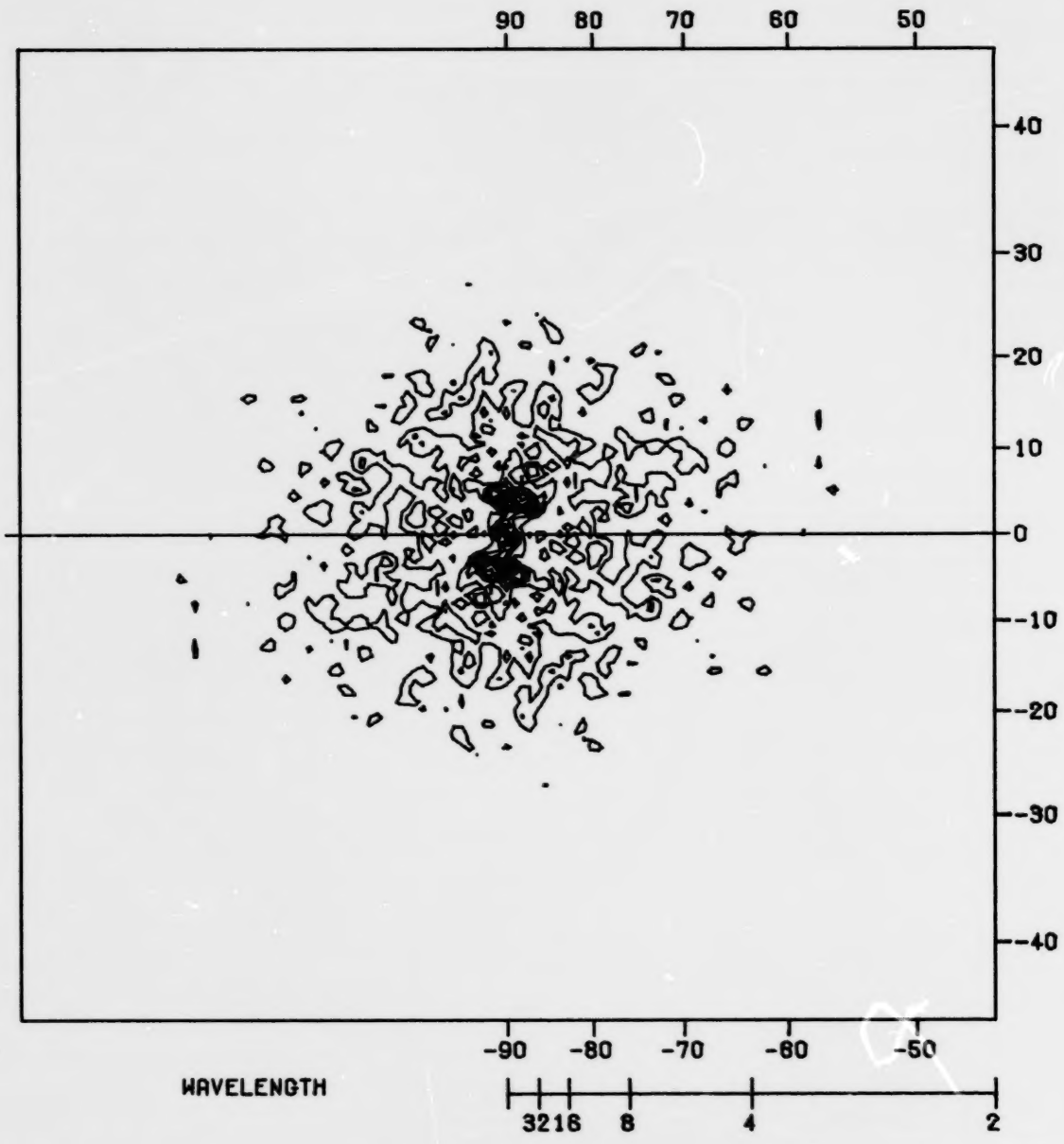

SAR 580 81-66-X1 CARTWRIGHT AVERAGED FFT FROM 10 SCENES DEC=2 RES=6

Figure 12

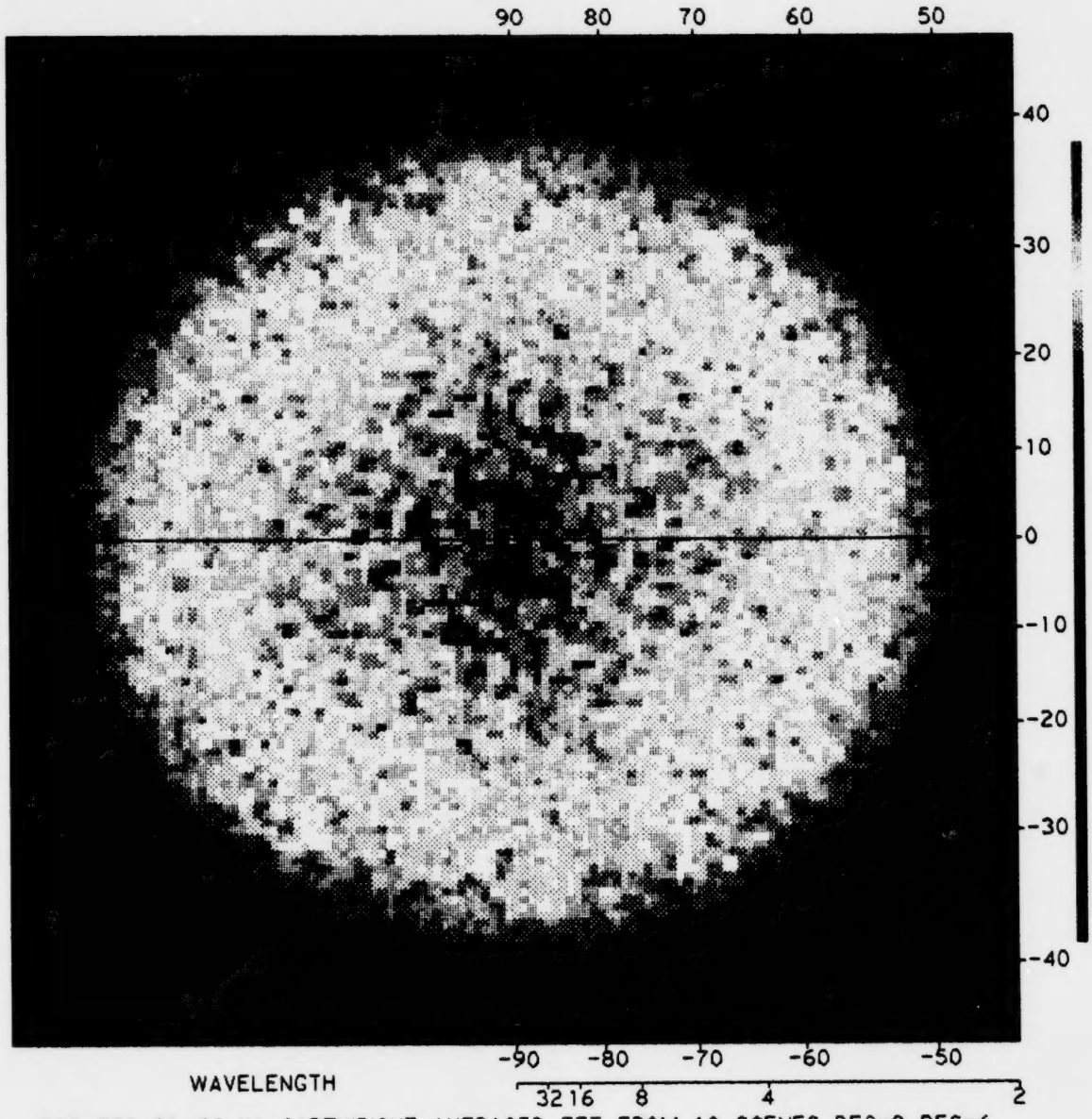
90
80
70
60
50
40
30
20
10
0
-10
-20
-30
-40
-90
-80
-70
-60
-50
WAVELENGTH
32 16
8
4
2
SAR 580 81-66-X1 CARTWRIGHT AVERAGED FFT FROM 10 SCENES DEC=2 RES=6

Figure 13

As suggested by the higher resolution analysis, there is a definite north-north-east trend in the positions of the peaks. There are two strong peaks, one at 190 m and 75° and the other at about 155 m and 56°. There also appears to be a peak at a very long wavelength tending at -45°, one pixel from the centre of the transform. Little more can be said about this peak.

The comparison of the one-dimensional spectra to the SAR transform is shown in Figure 14. A definite peak occurs in the SAR transform at about the same wavelength as is seen in the spectra from the waveriders. The peak in the SAR data, however, does not stand above the 95% confidence interval. No other peaks are evident in the SAR data.

OTHER MEASUREMENTS

It was unfortunate that the waverider buoys were not capable of extracting directional wave information from the measured wave field. This type of comparison will have to await the deployment of new directional buoys by MEDS.

There were, however, wind measurements made at about the same time as the SAR flight. These were logged every 30 minutes with 5 minute averages used to compute wind speed and direction. Table 2 shows the observations. Since there were no recording anemometers aboard the rigs, these are the best observations available. As can be seen, the winds were light and from the north-north-east gradually shifting to the north east. At 2200 when the SAR measurements were obtained, the winds were from 30° which corresponds very well with a qualitative estimate of the orientation of the waves as seen in Figure 4.

DISCUSSION AND SUMMARY

The results of analyses of the SAR data appear to be limited by a number of factors. First, the data appear to be noisy given that there are only about 25 independent values distributed over 3 orders of magnitude in the SAR signal. Secondly, the wind conditions were fairly light but steady. Since the wavelength of a SAR is on the order of a few centimeters, it is expected that a SAR is most sensitive to these short capillary waves generated by the wind. There should be some dependence on the strength of the SAR return on the wind speed. Thirdly, the significant wave height at the time of the SAR measurements was about 1.1 metres for the main peak of the waverider spectrum.

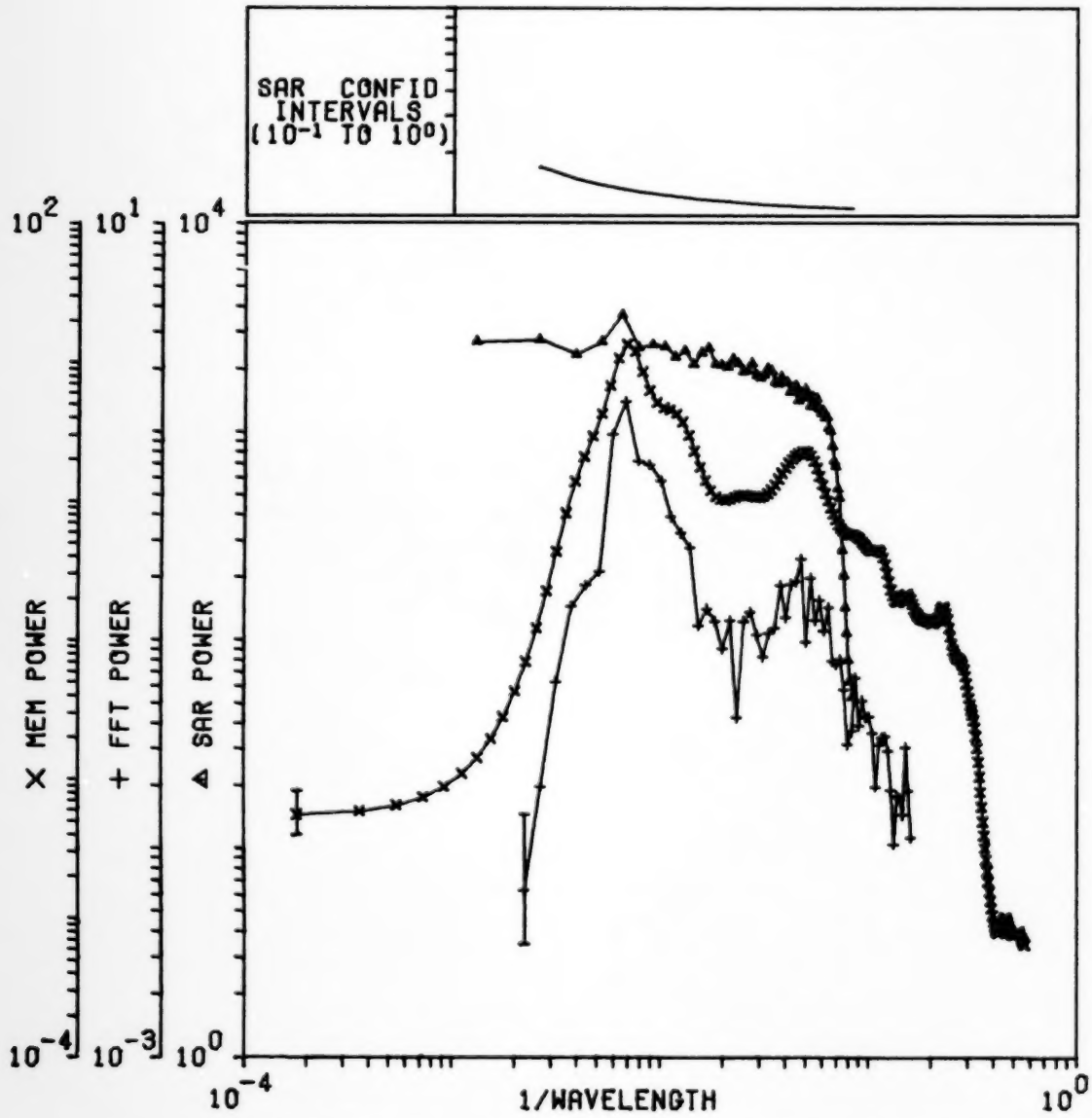
SAR CONFID INTERVALS (10-1 TO 10⁰)
10²
10¹
10⁴
× MEM POWER
+ FFT POWER
▲ SAR POWER
10⁻⁴
10⁻³
10⁰
10⁻⁴
1/WAVELENGTH
10⁰
SAR 580 81-66-X1 CARTWRIGHT AVERAGED FFT FROM 10 SCENES DEC=2 RES=6

Figure 14

Table 2. Wind observations collected from the Zapata Ugland on September 1, 1982.

Time (GMT)	Wind Speed (km/hr)	Wind Direction
2000	12.5	10
2030	14.5	10
2100	17.0	10
2130	16.0	20
2200	17.0	30

Given these factors, it may be encouraging that any correspondence between the SAR and waverider measurements was found.

Because directional information for the wave field was not measured, a quantitative evaluation of the SAR direction resolution abilities is not available. The wind data show directions of 10° gradually shifting to 30°. Visual estimates of directions from the SAR images show the same orientation of about 30°. The SAR data, however, show two components in the wave field, one at 15° and the other at about 35°. The latter corresponds reasonably with visual estimates and the final wind direction. The former is closer to the direction of the wind in the hours before the SAR data were obtained. A possible explanation for these two components may be advanced. If the waverider spectra from the 20 minute records prior to the SAR flight are examined, it can be seen that the wavelength of the peak in the spectra occurs at about 170 m. This is closer to the wavelength of one of the peaks in the two-dimensional SAR transform. As well, this longer wavelength is in a direction closer to north which was also true of the direction of the wind prior to the SAR data collection. It would appear then, that a possible explanation of the dual peaks in the SAR transform is that the wave field is adjusting to a changing wind direction.

ACKNOWLEDGEMENTS

The author would like to thank Mobil Oil and Fenco for their cooperation in collection of the waverider and wind data. Thanks are also due to the Radarsat office for providing the opportunity to work on the program, for the provision of the aircraft and analyses of the SAR data. The CRC provided the geometrically corrected digital SAR data. Discussions with J. Taylor of MEDS were extremely valuable in accomplishing the writing of the necessary computer programs. Finally, thanks are necessary to R. Hanebury for his valuable assistance in the analyses of all of the data.

REFERENCES

Alpers, W.R., D.B. Ross and C.L. Reyenach. 1981. On the detectability of ocean surface waves by real and synthetic aperature radar. J. Geophys. Res., 86(C7): 6481-6498.

Beal, R.C. 1980. Spaceborne imaging radar: monitoring of ocean waves. Science, 208(20). 1373-1375.

Beal, R.C., P.S. DeLeonibus and I. Katz. 1981. (ed.) Spaceborne synthetic aperature radar for oceanography. John's Hopkins University Press.

Hanebury, G.R. and J.R. Keeley. 1982. Software documentation for deriving directional wave information from SAR imagery. Mar. Environ. Data Serv. (In press).

Hsiao, S.V. 1978. The comparison between the synthetic aperture radar imageries and the surface truth of ocean waves. Proceedings of the Ocean's '78 Conference, September 6-8: 385-389.

Taylor, J.D. 1982. Calculation of two-dimensional filters. Mar. Environ. Data Serv. Tech. Note. (In press).

Ulrych, T.J. and T.N. Bishop. 1975. Maximum entropy spectral analysis and autoregressive decomposition. Rev. Geophysics and Space Physics 13(1): 183-200.

Vesechy, J.F. and R.H. Stewart. 1982. The observation of ocean surface phenomena using imagery from the SEASAT synthetic aperture radar: an assessment. J. Geophys. Res. 87(C5): 3397-3430.

Wilson, J.R. and W.F. Baird. 1981. Canadian wave climate study organization and operation. Mar. Sci. Inform. Directorate. Dep. Fish. Oceans MS Rep. Ser. 59: 26 p.

POOR

QUALITY

ORIGINAL